

# AQ-PCDSys: An Adaptive Quantized Planetary Crater Detection System for Autonomous Space Exploration

Aditri Paul<sup>1</sup> and Archan Paul<sup>2</sup>

<sup>1</sup>Manipal University Jaipur, India. [aditripaul7@gmail.com](mailto:aditripaul7@gmail.com)

<sup>2</sup>Computational Scientist and Independent Researcher, India. [paularchan@gmail.com](mailto:paularchan@gmail.com)

## Abstract

Autonomous planetary exploration missions are critically dependent on real-time, accurate environmental perception for navigation and hazard avoidance. However, deploying deep learning models on the resource-constrained computational hardware of planetary exploration platforms remains a significant challenge. This paper introduces the Adaptive Quantized Planetary Crater Detection System (AQ-PCDSys), a novel framework specifically engineered for real-time, onboard deployment in the computationally constrained environments of space exploration missions. AQ-PCDSys synergistically integrates a Quantized Neural Network (QNN) architecture, trained using Quantization-Aware Training (QAT), with an Adaptive Multi-Sensor Fusion (AMF) module. The QNN architecture significantly optimizes model size and inference latency suitable for real-time onboard deployment in space exploration missions, while preserving high accuracy. The AMF module intelligently fuses data from Optical Imagery (OI) and Digital Elevation Models (DEMs) at the feature level, utilizing an Adaptive Weighting Mechanism (AWM) to dynamically prioritize the most relevant and reliable sensor modality based on planetary ambient conditions. This approach enhances detection robustness across diverse planetary landscapes. Paired with Multi-Scale Detection Heads specifically designed for robust and efficient detection of craters across a wide range of sizes, AQ-PCDSys provides a computationally efficient, reliable and accurate solution for planetary crater detection, a critical capability for enabling the next generation of autonomous planetary landing, navigation, and scientific exploration.

**Keywords:** Crater Detection, Deep Learning, Model Quantization, Attention Mechanisms, Computer Vision, Artificial Intelligence (AI), Real-Time Object Detection, Sensor Fusion, Autonomous Navigation, Space Exploration, Edge AI / Edge Computing

## 1 Introduction

The success of autonomous planetary missions, from the historic Apollo landings to the ambitious goals of the Artemis program, is fundamentally tied to the ability of a planetary exploration platform to perceive and understand its immediate surroundings in real-time. Planetary craters are not merely topographical features; they are a geological record, essential for age-dating planetary surfaces, studying stratigraphy, and identifying sites of scientific interest [1, 2]. For autonomous systems, planetary craters serve as essential fiducial markers for localization, terrain mapping, and hazard avoidance. The development of robust and computationally efficient detection solutions is crucial for enabling precise localization, safe terrain traversal, and effective hazard avoidance for platforms such as planetary landers, rovers, and orbital reconnaissance vehicles operating far from Earth-based control.

While individual components such as deep learning for crater detection, neural network quantization, and multi-sensor fusion are well-established, the innovation of AQ-PCDSys stems from the novel and synergistic integration of these distinct components. This meticulously engineered approach directly addresses the power, memory, and computational constraints intrinsic to space exploration systems operating in planetary environments, with every architectural decision driven by the primary requirement of enabling high-performance inference on the limited hardware available for deep

space missions. From an information-theoretic standpoint, the challenge is to maximize the extraction of salient feature information from high-bandwidth OI and DEM data streams under the severe computational constraints imposed by onboard systems. AQ-PCDSys is designed to be an optimal information-theoretic processor for this specific context.

To address this challenge, we propose the Adaptive Quantized Planetary Crater Detection System (AQ-PCDSys) [10]. This work makes the following primary contributions specifically optimized for planetary missions:

- The design of a highly efficient **Quantized Neural Network (QNN) architecture** trained using Quantization-Aware Training (QAT) to optimize model size and accelerate inference on the integer-arithmetic units of resource-constrained onboard processors with minimal accuracy degradation.
- The development of a novel **Adaptive Multi-Sensor Fusion (AMF) module** that intelligently integrates Optical Imagery (OI) and Digital Elevation Model (DEM) data, using a sophisticated **Adaptive Weighting Mechanism (AWM)** to dynamically learn and apply context-aware weights to each sensor modality. The AWM can be viewed as a learned, real-time approximation of Bayesian inference, where the network learns to estimate the posterior probability of a feature’s reliability given the ambient planetary context, thereby dynamically updating its ‘belief’ in each sensor’s contribution.
- The inclusion of **multi-scale detection heads**, which process the fused feature maps to enable robust and efficient detection of craters across a wide range of sizes, completing a synergistic framework optimized for real-time onboard deployment.

## 2 Related Work

Historically, conventional approaches to planetary crater detection have predominantly relied upon classical image processing techniques, including edge detection, morphological operations, and template matching [12, 13]. While these methodologies established foundational principles, they invariably exhibit significant limitations when confronted with the inherent complexities of the extraterrestrial environment. Such complexities encompass wide variations in illumination, exemplified by extreme shadows and high-sun glare; diverse crater morphologies, including fresh, degraded, overlapped, or partially buried formations; and intricate topographical variations. Consequently, these methods frequently necessitate extensive manual calibration and often yield inconsistent detection accuracies across varying datasets.

More recently, deep learning methodologies, particularly Convolutional Neural Networks (CNNs), have demonstrated superior capabilities by learning intricate hierarchical features directly from imagery. Two-stage detectors (e.g. Faster R-CNN [11]) achieve high accuracy by first proposing regions of interest and then classifying them. However, their computational demands make them unsuitable for onboard deployment. This has led to the adoption of single-stage detectors like the YOLO (You Only Look Once) series [6, 7]. While these models offer a better balance of speed and accuracy for real-time applications, they are not inherently suitable for the unique challenges of space exploration. Their reliance on ‘single-modality optical data’ makes them vulnerable to performance degradation in dynamic planetary conditions, and their standard full-precision implementation remains too computationally intensive for typical onboard resource-constrained hardware.

A significant impediment to deploying advanced deep learning models on autonomous planetary mission platforms is their substantial computational demand. Full-precision neural networks require extensive processing power and memory, rendering them impractical for the resource-constrained hardware on planetary landers and rovers. These onboard planetary mission platforms operate with strict power budgets, limited memory, and often lack the dedicated high-performance processing units common in ground-based workstations. Furthermore, a sole reliance on a single data modality can lead

to suboptimal performance in the dynamic and unpredictable environmental conditions prevalent on celestial bodies.

Consequently, a pressing unmet need exists for a sophisticated planetary crater detection system that can enable effective autonomous navigation. The critical challenge lies in simultaneously achieving three demanding requirements:

- exceptionally high accuracy in dynamic conditions,
- guaranteed real-time performance for immediate decision-making,
- and operational efficiency within the stringent power and memory budgets of planetary exploration platforms.

While some solutions exist, a system capable of concurrently satisfying these multifaceted criteria remains an open challenge within the current state-of-the-art. Addressing this technological deficit is anticipated to catalyze substantial advancements in the domain of autonomous planetary exploration.

### 3 System Architecture and Methodology

In response to the limitations delineated in the preceding analysis of related work, this section provides a detailed exposition of the AQ-PCDSys architecture and methodology. The system is characterized by a holistic design philosophy for real-time onboard deployment, wherein each architectural component is engineered in conjunction to ensure mutual reinforcement and optimal performance. The synergistic integration of a quantized neural network, adaptive multi-sensor fusion, and multi-scale detection is therefore a foundational principle of this framework. For instance, the computational efficiencies afforded by quantization are strategically leveraged to permit the implementation of a more sophisticated and robust adaptive fusion module without transgressing the stringent power constraints of the onboard hardware. Consequently, this tightly-coupled architecture is specifically engineered to achieve the requisite equilibrium between computational efficiency, operational robustness, and detection accuracy, which is essential for successful autonomous planetary exploration.

#### 3.1 System Overview and Operational Context

The AQ-PCDSys system operates as an integrated perception module within a broader autonomous navigation framework, as depicted in Figure 1. The architecture is designed to resolve the critical bottleneck of executing computationally intensive AI models on resource-constrained hardware typical of planetary exploration platforms.

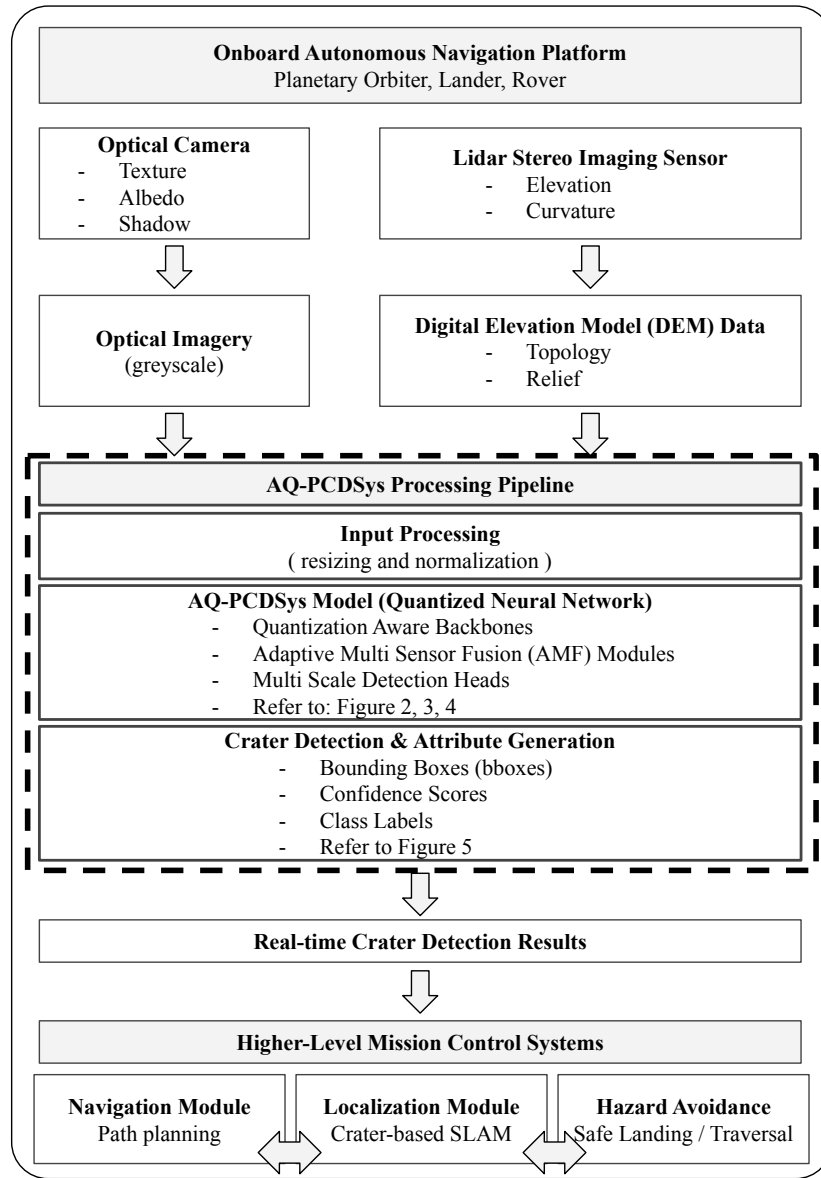


Figure 1: High-level architecture of the autonomous navigation platform, showing data flow from sensors through the AQ-PCDSys pipeline to mission control systems.

The operational pipeline starts with **Sensor Inputs**. Onboard optical cameras capture grayscale imagery, providing rich information on surface textures, albedo<sup>1</sup>, and shadows. Concurrently, LiDAR<sup>2</sup> (Light Detection and Ranging) or stereo-imaging sensors provide Digital Elevation Model (DEM) data, which offers precise topographical information that is invariant to illumination conditions. These continuous data streams are fed into the **AQ-PCDSys Processing Pipeline**. After initial preprocessing, the data enters the core AQ-PCDSys model, which performs the crater detection task in real-time. The output is a stream of crater attributes, including bounding boxes, confidence scores, and class labels. Finally, these detection results are transmitted instantaneously to **Higher-Level Mission Control Systems** on the autonomous platform, such as Navigation, Localization, and Hazard Avoidance modules, enabling real-time decision-making, which is crucial for mission success.

<sup>1</sup>Albedo refers to the measure of the diffuse reflectivity of a surface, indicating the proportion of incident light that it reflects rather than absorbs. In planetary science, variations in surface albedo are crucial for distinguishing geological features and understanding surface composition.

<sup>2</sup>LiDAR (Light Detection and Ranging) and stereo-imaging sensors are active and passive remote sensing technologies, respectively, used to acquire precise three-dimensional topographical data (Digital Elevation Models - DEMs). LiDAR emits pulsed lasers to measure distances, while stereo-imaging reconstructs 3D information from multiple 2D images captured from different perspectives. Both provide crucial depth and elevation data invariant to illumination conditions, essential for terrain mapping and hazard avoidance in planetary exploration.

### 3.2 Overall Model Architecture

The core of the system is a novel Quantized Neural Network, as illustrated in Figure 2. The architecture is a highly optimized design centered around a computationally-efficient, quantization-aware backbone. Its defining feature is the integration of Quantization-Aware Training (QAT), a sophisticated methodology that allows the network’s weights and activations to adapt to lower numerical precision, ensuring high accuracy while drastically reducing model size and accelerating inference speed. Crucially, this architecture incorporates an Adaptive Multi-Sensor Fusion (AMF) module that intelligently combines features from Optical Imagery (OI) and Digital Elevation Model (DEM) data using an Adaptive Weighting Mechanism (AWM). The AWM dynamically learns to prioritize the comparatively more reliable modality based on planetary ambient context, thereby significantly enhancing detection robustness. The fused multi-scale features are then processed by multi-scale detection heads, enabling accurate crater prediction across a wide range of sizes.

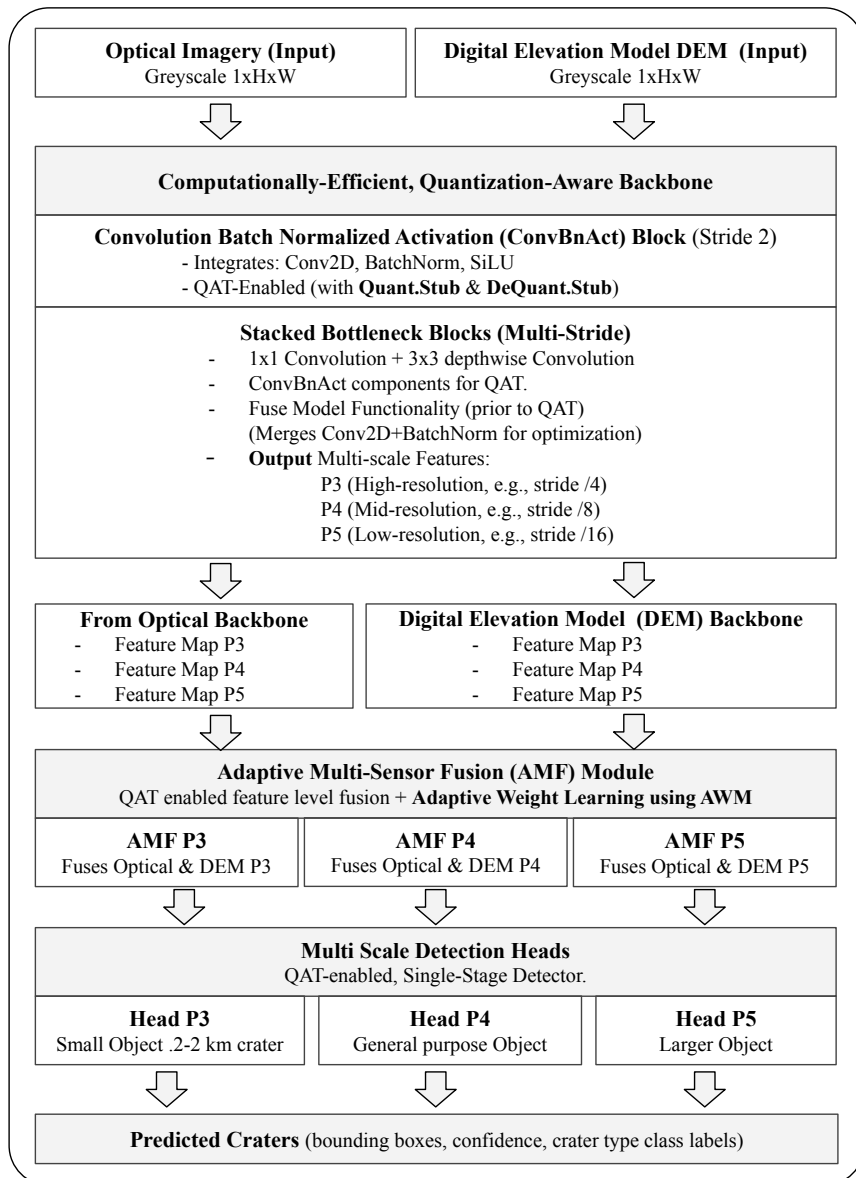


Figure 2: Block diagram of the AQ-PCDSys Quantized Neural Network, detailing the parallel backbones, AMF modules, and Multi-Scale Detection Heads.

### 3.3 Computationally-Efficient, Quantization-Aware Backbone

The backbone forms the efficient core of the architecture, engineered for a minimal parameter count and computational complexity. Its principal advancement is its suitability for **Quantization-Aware Training (QAT)** [4, 8]. This sophisticated training approach simulates lower numerical precision throughout the network, enabling the backbone’s weights and activations to adapt, ensuring high accuracy is preserved even when deployed as a fully quantized model. The core of QAT is the simulation of quantization, which maps a full-precision floating-point value  $r$  to a lower-precision integer  $q$ . This is achieved through an affine mapping:

$$r \approx S(q - Z) \quad (1)$$

where  $S$  is the scale factor (a positive float) and  $Z$  is the zero-point (an integer). The training process learns to adjust the network’s weights to be resilient to this quantization-dequantization process, minimizing accuracy loss.

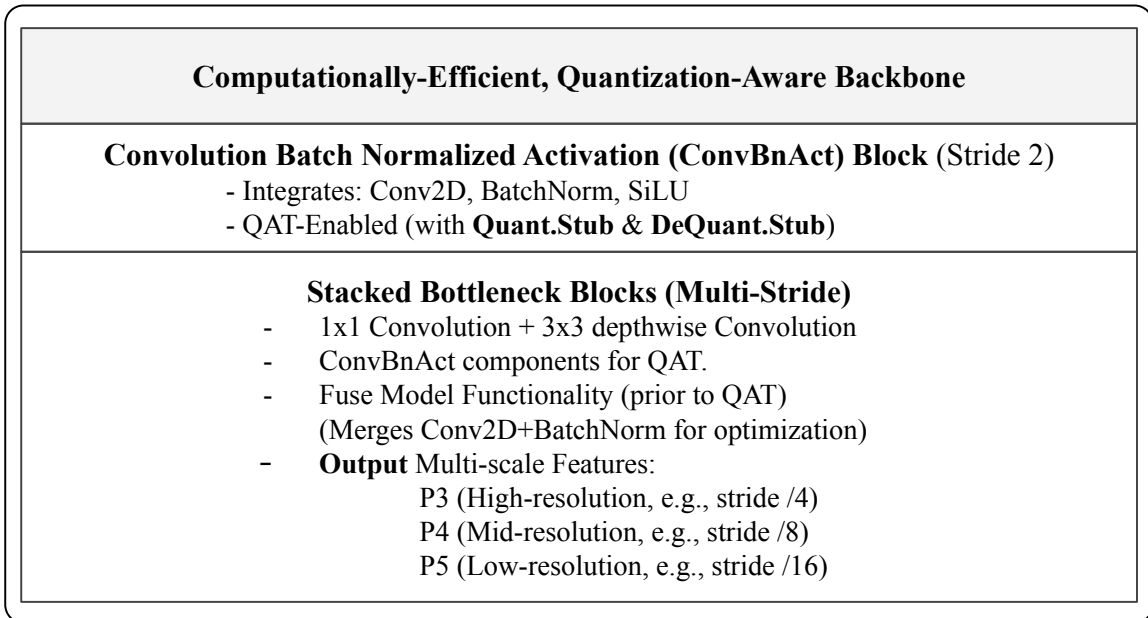


Figure 3: Block diagram of Quantization-Aware Backbone.

#### 3.3.1 Core Building Blocks of Backbone

The backbone is constructed from two main building blocks:

- **ConvBnAct Block:** This fundamental unit integrates a Conv2D<sup>3</sup> layer, a BatchNorm<sup>4</sup> layer, and a SiLU<sup>5</sup> activation function. The initial processing stage of the backbone is a ConvBnAct block with a stride of 2. This is a critical design choice for downsampling, as it reduces the spatial dimensions of the feature map by half, significantly decreasing the computational load

<sup>3</sup>Conv2D (2D Convolutional) layer is a fundamental building block in Convolutional Neural Networks (CNNs), which applies a set of learnable filters (kernels) to an input feature map to produce an output feature map.

<sup>4</sup>BatchNorm (Batch Normalization) is a technique used to stabilize learning in deep neural networks by normalizing the input to each layer, typically by adjusting and scaling the activations.

<sup>5</sup>SiLU (Sigmoid Linear Unit) is an activation function defined as  $f(x) = x \cdot \sigma(x)$ , where  $\sigma(x)$  is the sigmoid function. It introduces non-linearity into neural networks and is known for its smooth, non-monotonic properties, which contribute to improved convergence and performance in deep learning models.

on all subsequent layers. This downsampling is also the primary mechanism for creating the ‘hierarchical feature pyramid’, forcing the network to learn more abstract features as the spatial dimensions shrink. During QAT, these blocks are equipped with pseudo-quantization stubs that simulate the effects of lower numerical precision, enabling the network to adapt its weights for optimal quantization.

- **Stacked Bottleneck Blocks:** These compact units are deployed within the backbone. Each block typically comprises a 1x1 point-wise convolution followed by a 3x3 depthwise separable convolution, strategically designed to achieve efficient feature extraction with minimal computational cost. This factorization drastically reduces the number of parameters and multiply-accumulate (MAC)<sup>6</sup> operations compared to a standard convolution, making it ideal for resource-constrained hardware. By incorporating “ConvBnAct” components and applying Quantization-Aware Training (QAT) principles, these stacked blocks are crucial for efficiently generating the multi-scale feature maps (P3, P4, P5) that form the basis of the detection heads.

### 3.3.2 Fuse Model Functionality

Prior to QAT, a Fuse Model method is invoked across the network’s sequential blocks. This crucial process merges eligible layers (e.g., Conv2d and BatchNorm2d) into a single, optimized module. During inference, a standard convolutional layer is followed by a separate batch normalization step, each requiring its own memory access and computational kernel call. By mathematically folding the batch normalization parameters into the weights and biases of the preceding convolutional layer, these two operations can be combined into a single, fused convolutional layer. This fusion significantly reduces computational overhead by eliminating intermediate memory transfers and is essential for achieving effective hardware acceleration during subsequent quantized inference, as many specialized processors can execute a fused convolution-normalization operation as a single, highly efficient instruction.

### 3.3.3 Multi-Scale Feature Maps

The backbone is engineered to output **Multi-Scale Feature Maps**, denoted as P3, P4, and P5. In object detection architectures employing Feature Pyramid Networks (FPNs), the ‘P’ signifies ‘Pyramid’, referring to the distinct levels of the feature pyramid. The numerical designations correspond to the stride or total downsampling factor of the feature map relative to the original input.

- **P3 features** correspond to a feature map with a total stride of /4. This level balances high resolution with sufficient semantic information, making it ideal for detecting small objects.
- **P4 features** correspond to a stride of /8, suitable for medium-sized objects.
- **P5 features** correspond to a stride of /16. This level is coarser but semantically richer, making it effective for detecting large objects.

The generation of features at these multiple scales is crucial because it allows the network to capture information at varying levels of detail, enabling robust detection of craters across a wide range of sizes. These parallel sets of category wise feature maps, one derived from the Optical Imagery (OI) and the other from the Digital Elevation Model (DEM), serve as the direct inputs to the subsequent Adaptive Multi-Sensor Fusion module.

---

<sup>6</sup>Multiply-Accumulate (MAC) operation is a fundamental computational step consisting of a multiplication followed by an addition, where the product is added to a running total (accumulator). In the context of this research paper, MAC operations are a primary metric for quantifying computational complexity and directly determine the power consumption and latency of neural network inference on embedded processors, particularly in the discussion of optimizing depthwise separable convolutions for resource-constrained hardware.

### 3.4 Adaptive Multi-Sensor Fusion (AMF) Module

To bolster detection robustness, the system includes an Adaptive Multi-Sensor Fusion (AMF) Module. Operating on the parallel P3, P4, and P5 feature maps generated by the OI and DEM backbones, this module intelligently consolidates complementary information at the feature-level, as shown in Figure 4. This strategic fusion addresses a significant limitation inherent in single-modality sensing, which often struggles in the complex and variable environments of planetary missions. By combining the visual information from Optical Imagery with the topographical information provided by DEM data, the AMF module enables a more complete and accurate understanding of the planetary surface, mitigating the contextual limitations/weaknesses of each individual sensor.

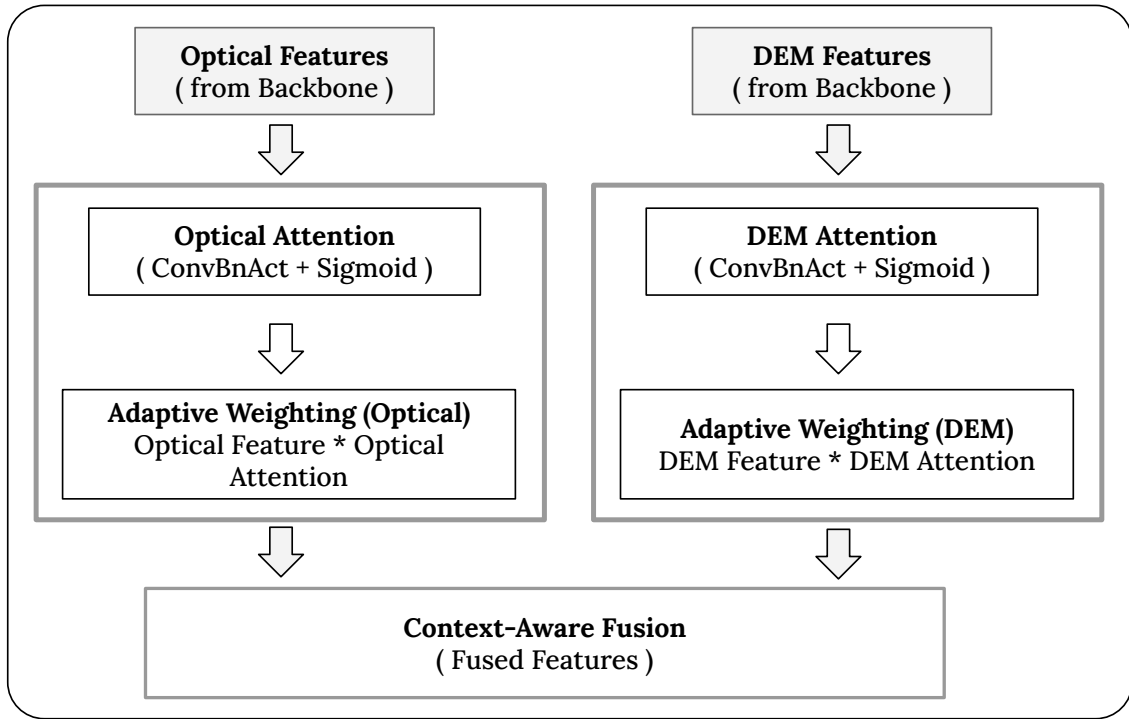


Figure 4: Detailed block diagram of the Adaptive Multi-Sensor Fusion (AMF) module, illustrating the attention sub-networks for OI and DEM data.

The module’s operation is defined by three key stages:

1. **Parallel Feature Extraction:** The system consists of two distinct, parallel feature extraction branches (Optical Feature branch and DEM Feature branch), each comprising a computationally-efficient, quantization-aware backbone. The Optical Feature branch processes the grayscale optical image, extracting textural details, albedo variations, and shadow patterns. The DEM Feature branch processes the single-channel DEM data, focusing on topographical cues such as elevation changes, slopes, and curvature, which are invariant to illumination.
2. **Adaptive Weighting Mechanism (AWM):** Central to the adaptive functionality of the AMF, this mechanism processes each feature map from the parallel modality branches (e.g., Optical-P3 & DEM-P3; Optical-P4 & DEM-P4; Optical-P5 & DEM-P5) through a dedicated sub-network to generate an attention map. This sub-network, typically structured with a ConvBnAct block, a 1x1 convolution, and a Sigmoid activation function, generates an Attention Map / Weighting Mask specifically tailored for its respective sensor modality. For example, in planetary regions characterized by profound shadows, where optical intensity values are diminished, the model is configured to learn and subsequently apply higher weights to the “DEM

features” and proportionally lower weights to the “Optical features”, thereby leveraging the DEM’s invariant depth information. Conversely, within well-illuminated, “geologically uniform mare regions” where DEM data may offer reduced discriminative information, the optical feature branch may consequently receive a higher weighting due to its superior textural content. This adaptive weighting ensures optimal feature emphasis contingent upon prevailing ambient conditions.

3. **Feature-Level Fusion:** The generated **attention maps** are applied multiplicatively to their corresponding feature maps (e.g.,  $Feature_{optical} \times Attention_{optical}$ ,  $Feature_{dem} \times Attention_{dem}$ ). Subsequently, these weighted features from both modalities are combined, typically through element-wise summation or concatenation, to yield a unified, fused feature map. This composite representation provides a richer, more robust understanding of the planetary surface, which is then passed to the detection heads.

This adaptive fusion mechanism empowers AQ-PCDSys to harness the complementary strengths of optical and topographic data, culminating in more robust and accurate crater detection, especially for ambiguous or partially obscured craters that might be missed by single-modality approaches.

### 3.4.1 Adaptive Weighting Mechanism (AWM)

Central to the AMF is the **Adaptive Weighting Mechanism (AWM)**, a sophisticated deep learning component critical for autonomous navigation. This mechanism is meticulously designed to dynamically regulate the influence of diverse sensor modalities on the fused feature representation. Its primary function is to enable the network to intelligently prioritize information from the most relevant and dependable sensor sources, adapting seamlessly to varying ambient conditions. This methodology signifies a substantial departure from conventional approaches that rely on static, predefined weights, which frequently prove inadequate in accounting for the unpredictable and dynamic nature of space environments.

The core principle is that the contribution of each sensor is not constant. For instance, optical data is highly informative in well-lit areas but becomes unreliable in deep shadows. In such scenarios, topographical information from a DEM, which is invariant to illumination, becomes paramount. The AWM allows the system to make this contextual determination autonomously through learned parameters. This is achieved through small, dedicated ‘Attention Sub-Networks’ for each sensor modality, a concept inspired by foundational attention mechanisms [14].

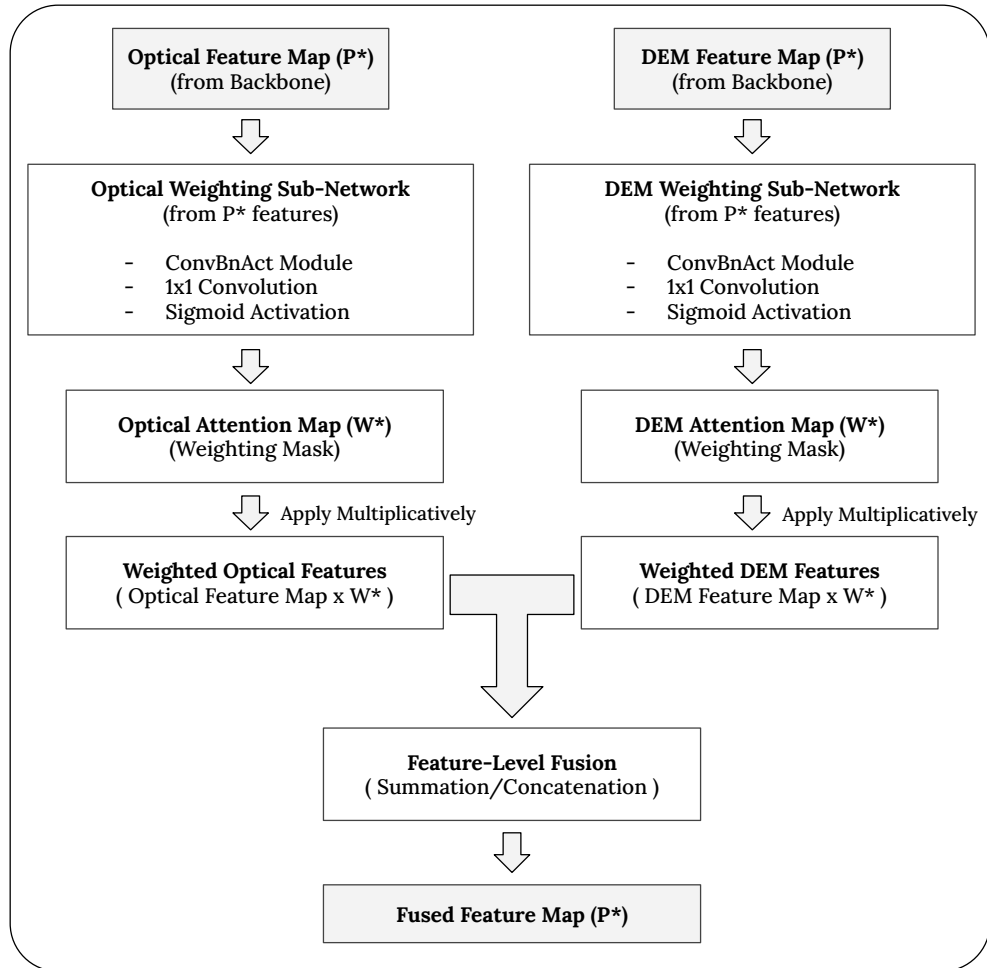


Figure 5: Flowchart of Adaptive Weighting Mechanism (AWM).

Let  $F_{oi} \in \mathbb{R}^{C \times H \times W}$  and  $F_{dem} \in \mathbb{R}^{C \times H \times W}$  be the feature maps from the Optical and DEM backbones, respectively. The attention maps  $A_{oi}$  and  $A_{dem}$  are generated by dedicated sub-networks:

$$A_{oi} = \sigma(\text{Conv}_{oi}(F_{oi})) \quad (2)$$

$$A_{dem} = \sigma(\text{Conv}_{dem}(F_{dem})) \quad (3)$$

where Conv represents the attention sub-network (e.g., ConvBnAct + 1x1 Conv) and  $\sigma$  is the sigmoid activation function, which scales the weights between 0 and 1.

The weighted features are then computed via element-wise multiplication ( $\odot$ ):

$$F_{\text{weighted\_oi}} = A_{oi} \odot F_{oi} \quad (4)$$

$$F_{\text{weighted\_dem}} = A_{dem} \odot F_{dem} \quad (5)$$

Finally, the fused feature map,  $F_{\text{fused}}$ , is produced by a combination operator, such as concatenation or summation. This process is formalized in Algorithm 1.

---

**Algorithm 1** Adaptive Weighting Mechanism (AWM)

---

**Require:** Optical Feature Map  $F_{oi}$ , DEM Feature Map  $F_{dem}$

**Ensure:** Fused Feature Map  $F_{\text{fused}}$

- 1: ▷ Generate attention maps.
  - 2:  $A_{oi} \leftarrow \text{AttentionSubNetwork}_{oi}(F_{oi})$
  - 3:  $A_{dem} \leftarrow \text{AttentionSubNetwork}_{dem}(F_{dem})$
  - 4: ▷ Apply weights.
  - 5:  $F_{\text{weighted\_oi}} \leftarrow F_{oi} * A_{oi}$
  - 6:  $F_{\text{weighted\_dem}} \leftarrow F_{dem} * A_{dem}$
  - 7: ▷ Fuse features.
  - 8:  $F_{\text{fused}} \leftarrow \text{Concatenate}(F_{\text{weighted\_oi}}, F_{\text{weighted\_dem}})$
  - 9: **return**  $F_{\text{fused}}$
- 

A pivotal characteristic of AQ-PCDSys is its capacity for **Adaptive Learning**. The attention sub-networks contain tunable parameters, specifically, the weights of their convolutional layers, that are optimized via the backpropagation algorithm during Quantization-Aware Training (QAT). The gradients computed from the holistic, system-level Loss Function flow backward through the entire architecture, including these attention sub-networks. This allows their parameters to be iteratively updated to minimize the overall detection error, implicitly training the AWM to generate optimal, context-sensitive weights. This adaptive, learned weighting mechanism is crucial for enhancing the model’s robustness and its ability to generalize to unseen data. It allows the system to dynamically adjust feature importance, mitigate the impact of sensor-specific noise, and adapt to evolving environmental conditions. In essence, the AWM transforms static multi-sensor fusion into an intelligent, context-aware integration process, which is indispensable for reliable, real-time operation.

### 3.5 Multi-Scale Detection Heads

The **Multi-Scale Detection Heads** in the AQ-PCDSys architecture are the specialized components responsible for processing the high-level, fused feature maps and predicting the final crater attributes. These heads operate on feature maps from different feature pyramid levels (P3, P4, P5), which correspond to progressively coarser spatial resolutions (strides of /4, /8, and /16, respectively) but richer semantic information. They are designed with a single-stage, regression-based detector architecture, which directly predicts outputs in a single pass, and are enabled for Quantization-Aware Training (QAT). This design significantly reduces computational complexity and memory footprint, facilitating high-speed inference on the resource-constrained hardware used onboard planetary exploration missions.

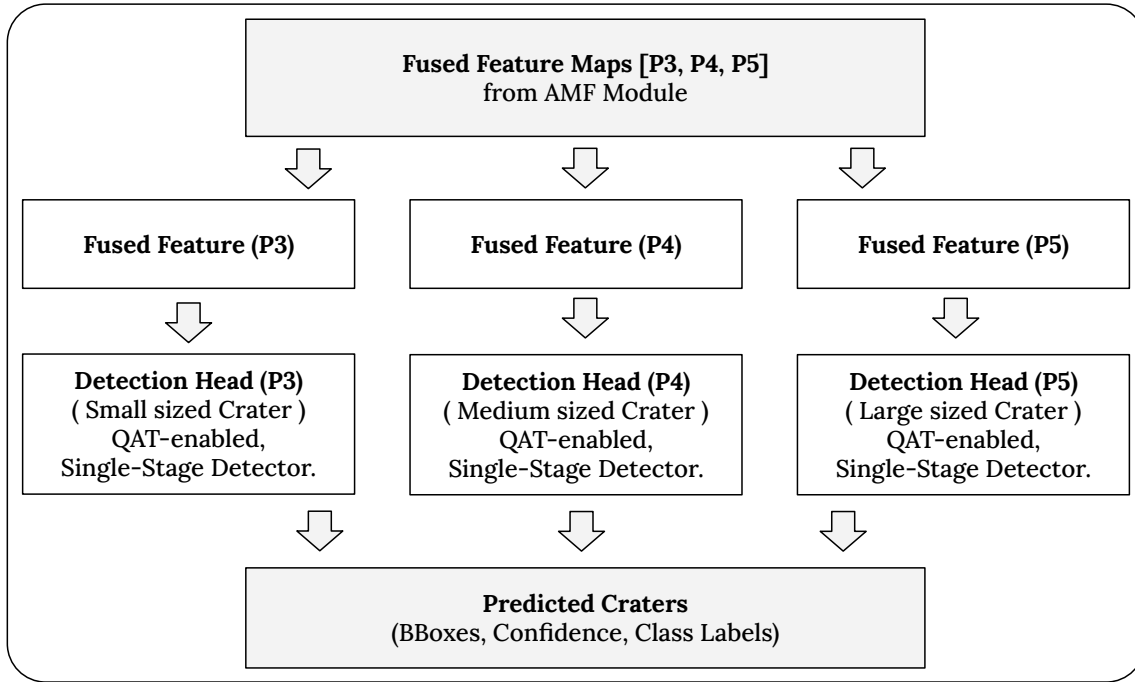


Figure 6: Flowchart of the Multi-Scale Detection Heads, showing how fused feature maps (P3, P4, P5) are processed by specialized heads to detect craters of different sizes.

The Multi-Scale aspect signifies that there are separate detection heads operating on feature maps of varying resolutions. This is crucial for effectively detecting craters of different sizes, as the P3, P4, and P5 levels achieve an optimal balance between spatial resolution and semantic richness:

- **Head P3 (stride /4):** Operates on the highest-resolution feature map (P3), with a dedicated focus on small craters (0.2 to 2 km). This head is optimized to capture the fine-grained spatial information necessary for accurately resolving these challenging targets, which are often difficult to detect but critical for hazard avoidance.
- **Head P4 (stride /8):** A general-purpose head that processes the mid-resolution P4 feature map to detect medium-sized craters.
- **Head P5 (stride /16):** Operates on the lowest-resolution, semantically rich P5 feature map to detect large craters and basins, which serve as key landmarks for global localization.

The integration of these optimized heads with the adaptively fused features ensures robust detection across the full range of crater sizes, from large basins to small, subtle formations. This comprehensive approach enhances the system’s precision and utility for autonomous navigation.

## 4 Training Methodology and Deployment

The AQ-PCDSys model undergoes a rigorous training regimen utilizing Quantization-Aware Training (QAT) on a composite dataset derived from publicly available, scientifically validated sources. For lunar applications, the training data comprises high-resolution Optical Imagery from the Lunar Reconnaissance Orbiter Camera (LROC), Narrow Angle Camera (NAC) instruments, precisely co-registered with corresponding Digital Elevation Model (DEM) data from the Lunar Orbiter Laser Altimeter (LOLA). For Martian contexts, data from the High Resolution Imaging Science Experiment (HiRISE) and the Mars Orbiter Laser Altimeter (MOLA) are used. To ensure robustness against the

highly variable ambient conditions encountered on planetary surfaces, the training dataset is extensively augmented. This augmentation process includes simulating a wide range of solar illumination angles (e.g., from  $5^\circ$  to  $85^\circ$ ) to create diverse shadow patterns, as well as incorporating examples of various crater morphologies, including fresh, degraded, and overlapping formations. This integrated training ensures that the model acquires the capability to effectively extract features and fuse information directly within the quantized domain, preparing it for low-precision inference.

The training is driven by a meticulously designed **Composite Loss Function**. The total loss is calculated as the sum of the losses from each detection head (P3, P4, P5). Each head’s loss ( $L_{P_x}$ ) is a weighted sum of three critical components:

- **Localization Loss ( $L_{loc}$ ):** This loss guides the model in precisely predicting the bounding box coordinates and dimensions. It is often implemented as a Complete Intersection over Union (CIoU)<sup>7</sup> loss, which penalizes differences in overlap area, central point distance, and aspect ratio between the predicted and ground-truth boxes.
- **Objectness Confidence Loss ( $L_{obj}$ ):** This loss assesses the model’s certainty regarding the presence or absence of a crater within a proposed region. It is typically a Binary Cross-Entropy (BCE)<sup>8</sup> loss that teaches the model to distinguish between true positive detections and background noise.
- **Classification Loss ( $L_{cls}$ ):** This loss enables the model to accurately categorize detected objects as craters. For this single-class detection problem, it is also a BCE loss that measures how well the model’s prediction matches the ground-truth label.

The loss for each head is thus formulated as:

$$L_{P_x} = \lambda_{loc} \cdot L_{loc} + \lambda_{obj} \cdot L_{obj} + \lambda_{cls} \cdot L_{cls} \quad (6)$$

A unique and crucial aspect of this training methodology is the strategic application of an additional **‘Loss Boost’**. This boost is *specifically* applied to the loss calculated by the P3 detection head, which is responsible for small, challenging-to-detect craters. This is achieved by introducing a weighting hyperparameter ( $w_s > 1$ ), to the P3 head’s loss component ( $L_{P3}$ ). The final total loss is therefore calculated as:

$$L_{total} = (w_s \cdot L_{P3}) + L_{P4} + L_{P5} \quad (7)$$

By amplifying the error signal for these critical small-crater instances ( $w_s \cdot L_{P3}$ ), the model is compelled to dedicate more learning capacity to refine its understanding of these fine-grained features, preventing them from being overlooked in favor of larger, easier-to-detect craters.

The training regimen incorporates an **Adaptive Learning Rate scheduler**, which dynamically adjusts the learning rate to optimize convergence. A common approach is Exponential Decay<sup>9</sup>, where the learning rate  $lr$  at epoch  $e$  is given by:

$$lr(e) = lr_0 \cdot \gamma^{(e/d)} \quad (8)$$

where  $lr_0$  is the initial learning rate,  $\gamma$  is the decay rate, and  $d$  is the number of decay steps. This

<sup>7</sup>Complete Intersection over Union (CIoU) loss is a bounding box regression loss function used in object detection to measure the similarity between predicted and ground-truth bounding boxes. Beyond simply penalizing the non-overlapping area (as in IoU), CIoU loss also considers the distance between central points and the consistency of aspect ratios, leading to more accurate and stable bounding box predictions.

<sup>8</sup>Binary Cross-Entropy (BCE) loss is a widely used loss function in machine learning, particularly for binary classification tasks. It quantifies the difference between two probability distributions, the predicted probabilities from the model and the true binary labels.

<sup>9</sup>Exponential Decay is a method used within an adaptive learning rate scheduler to progressively reduce the learning rate during neural network training. The parameters are tuned for the optimization of convergence, preventing oscillations around the minimum which ensures that the model settles into a stable, accurate state during QAT.

is often coupled with an **Adam**<sup>10</sup> or **AdamW**<sup>11</sup> optimizer and early stopping mechanisms, which prevent overfitting by halting training when validation performance no longer improves.

Following the successful completion of the QAT process, the trained model undergoes conversion into a fully quantized format. This quantized model, distinguished by its significantly reduced size and enhanced inference speed, is exceptionally well-suited for deployment on resource-constrained onboard computing systems of space exploration missions, such as orbiters, landers, and rovers. These platforms encompass, but are not restricted to, space-qualified, power-efficient micro-controllers, micro-processors, and specialized Artificial Intelligence (AI) accelerators capable of executing mathematical operations at high velocities with optimal power consumption.

## 5 System Analysis and Discussion

The architectural design of AQ-PCDSys is grounded in established principles intended to address the unique challenges of onboard planetary crater detection. The efficacy of the system does not arise from a single component, but rather from the synergistic interplay between its constituent parts: the efficient quantized backbone, the context-aware adaptive fusion module, and the specialized multi-scale detection heads. This section analyzes the theoretical underpinnings of this synergy, focusing on computational complexity, the system’s positioning within the Edge AI operational trade-space, and the resulting architectural robustness that makes it suitable for high-stakes autonomous missions.

### 5.1 Computational Complexity Analysis

The computational viability of AQ-PCDSys on resource-constrained hardware is fundamentally rooted in the efficiency of its backbone, which primarily utilizes depthwise separable convolutions. A standard 2D convolution exhibits a computational cost of approximately  $O(K^2 \cdot C_{in} \cdot C_{out} \cdot H \cdot W)$ , where  $K$  is the kernel size. In contrast, a depthwise separable convolution factorizes this operation into two steps: a depthwise convolution followed by a pointwise convolution, with a combined computational cost of  $O(K^2 \cdot C_{in} \cdot H \cdot W + C_{in} \cdot C_{out} \cdot H \cdot W)$ . In these formulations,  $K$  represents the kernel size,  $C_{in}$  is the number of input channels,  $C_{out}$  is the number of output channels, and  $H$  and  $W$  are the height and width of the feature map, respectively.

This factorization yields a significant theoretical reduction in the required Multiply-Accumulate (MAC) operations, which is a primary determinant of power consumption and latency on embedded processors. This architectural choice provides a foundational layer of efficiency, which is further amplified by the subsequent quantization to integer arithmetic, making the entire perception pipeline feasible within the stringent operational envelopes of planetary exploration platforms.

### 5.2 The Edge AI Trilemma in a Space Context

The design of AQ-PCDSys represents a deliberate and optimized solution to the ‘Edge AI Trilemma’, the inherent trade-off between **accuracy, latency, and power consumption** that governs all edge computing applications. In the high-stakes context of space exploration, this trilemma is particularly acute, as mission success can depend on maximizing all three vertices simultaneously. AQ-PCDSys navigates this trade-space through a multi-faceted strategy:

- **Power Consumption** is directly minimized by employing QAT, which converts power-intensive 32-bit floating-point operations into more efficient 8-bit integer arithmetic.

<sup>10</sup>Adam (Adaptive Moment Estimation) optimizer is a widely used stochastic optimization algorithm for training deep neural networks. It combines the advantages of AdaGrad and RMSProp by computing adaptive learning rates for each parameter, maintaining exponentially decaying averages of past gradients (first moment) and past squared gradients (second moment).

<sup>11</sup>AdamW optimizer is a variant of the Adam optimization algorithm that decouples weight decay from the L2 regularization term, addressing a known issue where standard Adam’s adaptive learning rates can diminish the effectiveness of weight decay. This decoupling often leads to improved generalization performance and more robust training, especially in models with regularization.

- **Latency** is reduced by the computationally lightweight backbone architecture, which minimizes the number of required MAC operations per inference.
- **Accuracy and Robustness** are enhanced by the AMF module, which leverages multi-modal data to produce reliable detections even in sensor-degrading conditions.

The synergistic integration of these components allows AQ-PCDSys to occupy a highly favorable position within this trade-off space, one that is specifically optimized for the unique and unforgiving constraints of planetary missions.

### 5.3 Architectural Synergy and Robustness

The robustness of AQ-PCDSys is not merely an attribute but an emergent property of its integrated design. The choice of QAT is critical for onboard deployment; by converting FP32 operations to INT8, memory bandwidth requirements are reduced by a factor of four, a critical advantage on systems with limited memory buses and caches. This efficiency gain enables the allocation of computational resources to the more complex AMF module without violating the system’s overall power budget. The AMF module, in turn, provides crucial robustness against variable environmental conditions. For instance, in the permanently shadowed regions near the lunar poles, where temperatures can plummet and long, deep shadows obscure terrain, optical sensors are rendered ineffective. The AWM in AQ-PCDSys is designed to learn this context during training and automatically up-weight the contribution of features from the DEM data, which provides reliable topographical information independent of illumination. Concurrently, the multi-scale detection heads, particularly the dedicated P3 head for small objects (0.2-2 km), ensure that the system does not sacrifice performance on these challenging but navigationally vital features. This holistic design directly addresses the core challenge of deploying advanced AI on resource-constrained, radiation-hardened space hardware, providing a viable pathway to migrate complex perception tasks from earth-based analysis to the autonomous platforms actively exploring our solar system.

## 6 Conclusion and Future Work

### 6.1 Conclusion

This paper introduced AQ-PCDSys, a holistic computational framework and architectural blueprint for planetary crater detection, meticulously designed for the stringent constraints of autonomous space missions. By synergistically combining Quantization-Aware Training, an Adaptive Multi-Sensor Fusion module, and Multi-Scale Detection heads, the system presents a paradigm for co-designing perception algorithms with the operational realities of resource-constrained hardware. The architecture provides a theoretically robust solution to the Edge AI trilemma; balancing accuracy, latency, and power in the high-stakes context of outer space. This research outlines a direct approach for transferring sophisticated AI-powered perception capabilities from earth-based analysis to the autonomous planetary exploration systems.

### 6.2 Limitations and Immediate Future Work: Empirical Validation

The present work has focused on the architectural design and theoretical justification of the AQ-PCDSys framework. While the design is grounded in established principles, the immediate and most critical next step is to move from the proposed architecture to rigorous empirical validation. Our future work is therefore centered on implementing and benchmarking the system to quantitatively substantiate its performance. This plan involves the following key objectives:

- **Performance Benchmarking on Target Hardware:** The primary goal is to deploy the AQ-PCDSys model on space-qualified, radiation-hardened hardware and perform a comprehensive performance analysis. We will measure key metrics including detection accuracy (mAP, F1-score), inference latency (ms/frame), and power consumption (watts) under realistic operational scenarios.

- **Comparative Analysis:** To validate the effectiveness of our approach, we will conduct a direct comparative analysis against other state-of-the-art, lightweight object detection models (e.g., a quantized YOLO or MobileNet-SSD). This will establish a clear performance-per-watt baseline and demonstrate the advantages of the AQ-PCDSys architecture.
- **Ablation Studies:** To scientifically verify the contribution of each novel component, we will conduct a series of ablation studies. These experiments will systematically isolate the impact of the Adaptive Multi-Sensor Fusion (AMF) module, the Adaptive Weighting Mechanism (AWM), and the small-object loss boost on overall system accuracy and robustness.

### 6.3 Long-Term Research Directions

Following the successful completion of the empirical validation phase, we plan to explore several long-term research avenues:

- **Generalization to Other Geological Features:** We will investigate the transferability of the learned fusion strategies to detect other features of scientific interest, such as boulders, rilles, or potential landing hazards, thereby creating a more comprehensive terrain analysis tool.
- **Multi-Mission and Multi-Body Applicability:** We will conduct a systematic study of the AWM's behavior on bodies with significant atmospheric interference, to quantify its robustness to different sensor noise profiles and environmental conditions, further refining the system for broad, multi-mission applicability.

## Declarations

- **Funding:** The authors did not receive support from any organization for the submitted work.
- **Conflicts of interest:** The authors have no relevant financial or non-financial interests to disclose.

## References

- [1] Fassett, C., et al. “Lunar impact basins: Stratigraphy, sequence and ages from superposed crater populations measured from Lunar Orbiter Laser Altimeter (LOLA) data.” *J. Geophys. Res. Planets* 117.E12 (2012).
- [2] Head, J. W., et al. “Global distribution of large lunar craters: Implications for resurfacing and impactor populations.” *Science* 329.5998 (2010): 1504-1507.
- [3] He, K., et al. “Mask R-CNN.” *Proceedings of the IEEE international conference on computer vision* (2017): 2961-269.
- [4] Jacob, B., et al. “Quantization and training of neural networks for efficient integer-arithmetic-only inference.” *Proceedings of the IEEE conference on computer vision and pattern recognition* (2018): 2704-2713.
- [5] Jia, Y., Liu, L., Zhang, C. “Moon crater detection using nested attention mechanism based UNet++.” *IEEE Access* 9 (2021): 44107-44116.
- [6] Jocher, G., et al. “ultralytics/yolov5: v3.1 - Bug Fixes and Performance Improvements.” *Zenodo* (2020).
- [7] Redmon, J., et al. “You Only Look Once: Unified, Real-Time Object Detection.” *Proceedings of the IEEE conference on computer vision and pattern recognition* (2016): 779-788.
- [8] Krishnamoorthi, R. “Quantizing deep convolutional networks for efficient inference: A survey.” *arXiv preprint arXiv:1806.08342* (2018).
- [9] Lin, X., et al. “Lunar Crater Detection on Digital Elevation Model: A Complete Workflow Using Deep Learning and Its Application.” *Remote Sensing* 14.3 (2022): 621.
- [10] Paul, A., et al. “AQ-PCDSys: Adaptive Quantized Planetary Crater Detection System for Autonomous Outer Space Planetary Exploration.” (2025), Patent Pending.
- [11] Ren, S., et al. “Faster R-CNN: Towards Real-Time Object Detection with Region Proposal Networks.” *Advances in neural information processing systems* 28 (2015).
- [12] Salamunićar, G., & Lončarić, S. “Manual feature extraction in lunar studies.” *Computers & Geosciences* 34.10 (2008): 1217-1228.
- [13] Zuo, W., et al. “Contour-based automatic crater recognition using digital elevation models from Chang’E missions.” *Computers & Geosciences* 97 (2016): 79-88.
- [14] Vaswani, A., et al. “Attention is all you need.” *Advances in neural information processing systems* 30 (2017).